Generalized Thermalization in Quantum-Chaotic Quadratic Hamiltonians

Patrycja Łydżba, Marcin Mierzejewski, Marcos Rigol, and Lev Vidmar

Phys. Rev. Lett. **131**, 060401 — Published 8 August 2023

DOI: 10.1103/PhysRevLett.131.060401

Generalized Thermalization in Quantum-Chaotic Quadratic Hamiltonians

Patrycja Łydżba,[1] Marcin Mierzejewski,[1] Marcos Rigol,[2] and Lev Vidmar[3,4]

[1] *Department of Theoretical Physics, Wroclaw University of Science and Technology, 50-370 Wrocław, Poland*
[2] *Department of Physics, The Pennsylvania State University, University Park, Pennsylvania 16802, USA*
[3] *Department of Theoretical Physics, J. Stefan Institute, SI-1000 Ljubljana, Slovenia*
[4] *Department of Physics, Faculty of Mathematics and Physics, University of Ljubljana, SI-1000 Ljubljana, Slovenia*

Thermalization (generalized thermalization) in nonintegrable (integrable) quantum systems requires two ingredients, equilibration and an agreement with the predictions of the Gibbs (generalized Gibbs) ensemble. We prove that observables that exhibit eigenstate thermalization in single-particle sector equilibrate in many-body sectors of quantum-chaotic quadratic models. Remarkably, the same observables do not exhibit eigenstate thermalization in many-body sectors (we establish that there are exponentially many outliers). Hence, the generalized Gibbs ensemble is generally needed to describe their expectation values after equilibration, and it is characterized by Lagrange multipliers that are smooth functions of single-particle energies.

Introduction. The past 15 years, we have improved significantly our understanding of quantum dynamics in isolated many-body quantum systems [1–4]. A paradigmatic setup for these studies is the quantum quench, in which a sudden change of a tuning parameter pushes the system far from equilibrium. Following quantum quenches, observables in nonintegrable systems have been found to equilibrate to the predictions of the Gibbs ensemble (GE) [1, 5], while in integrable systems they have been found to equilibrate to the predictions of the generalized Gibbs ensemble (GGE) [6, 7]. The validity of the GGE has been tested in many theoretical studies of integrable models that are mappable onto quadratic ones [6–16], integrable models that are not mappable onto quadratic ones [17–28] (see Ref. [29] for reviews), and it is a starting point for the recently introduced [30, 31] and experimentally tested [32, 33] theory of generalized hydrodynamics.

Quadratic fermionic models, which are central to understanding a wide range of phenomena in condensed matter physics, can be thought as being a special (noninteracting) class of integrable models. Their Hamiltonians consist of bilinear forms of creation and annihilation operators. The infinite-time averages of one-body observables after quenches in these models are always described by GGEs [7, 34–36]. However, there are one-body observables that generically fail to equilibrate because the one-body density matrix evolves unitarily [37], i.e., generalized thermalization fails to occur. Such equilibration failures have been discussed in the context of localization in real [13, 34–36] and momentum [36, 37] space. Equilibration in quadratic models has been argued to occur for local observables in the absence of real-space localization. In particular, it has been shown to occur for initial states that are ground states of local Hamiltonians [38], as well as for initial states that exhibit sufficiently rapidly decaying correlations in real space [39–41].

In this Letter, we show that there is a broad class of quadratic fermionic models for which generalized thermalization is ensured by the properties of the Hamiltonian. Hence, it is robust and resembles (generalized) thermalization, which occurs in interacting (integrable) nonintegrable models. The class in question is that of quantum-chaotic quadratic (QCQ) Hamiltonians, namely, quadratic Hamiltonians that exhibit single-particle quantum chaos [42, 43]. Paradigmatic examples of local QCQ models are the three-dimensional (3D) Anderson model in the delocalized regime [42, 44] and chaotic tight-binding billiards [45], while their nonlocal counterparts include variants of the quadratic Sachdev-Ye-Kitaev (SYK2) model [46, 47] and the power-law random banded matrix model in the delocalized regime [46]. The single-particle sector of those models exhibits random-matrix-like statistics of the energy levels [44, 48, 49], as well as single-particle eigenstate thermalization [43], i.e., the matrix elements of properly normalized one-body observables $\hat{\mathcal{O}}$ [50] in the *single-particle* energy eigenkets are described by the eigenstate thermalization hypothesis (ETH) ansatz [1, 51]

$$\langle\alpha|\hat{\mathcal{O}}|\beta\rangle = \mathcal{O}(\bar{\epsilon})\delta_{\alpha\beta} + \rho(\bar{\epsilon})^{-1/2}\mathcal{F}_{\mathcal{O}}(\bar{\epsilon},\omega)R^{\mathcal{O}}_{\alpha\beta}\,, \quad (1)$$

where $\bar{\epsilon} = (\epsilon_\alpha+\epsilon_\beta)/2$, $\omega = \epsilon_\beta-\epsilon_\alpha$, $\mathcal{O}(\bar{\epsilon})$ and $\mathcal{F}_{\mathcal{O}}(\bar{\epsilon},\omega)$ are smooth functions of their arguments, and $\rho(\bar{\epsilon}) = \delta N/\delta\epsilon|_{\bar{\epsilon}}$ is the single-particle density of states (typically proportional to the volume) at energy $\bar{\epsilon}$. The distribution of matrix elements is described by the random variable $R^{\mathcal{O}}_{\alpha\beta}$, which has zero mean and unit variance. The *many-body* energy eigenstates, on the other hand, exhibit eigenstate entanglement properties typical of Gaussian states [42, 46, 47, 52, 53], see also [54].

We prove that single-particle eigenstate thermalization ensures equilibration in many-body sectors of QCQ Hamiltonians, and we also prove that eigenstate thermalization does not occur in those sectors. We then show that the GGE is needed to describe observables after equilibration, and that it is characterized by the Lagrange multipliers which are smooth functions of the single-particle energies. The latter is also a consequence of single-particle eigenstate thermalization. Our analytical results are tested numerically in QCQ Hamiltonians, and contrasted with results obtained for quadratic models that are not quantum chaotic.

Quantum quench and equilibration. We consider a quantum quench setup; the system is prepared in an initial many-body pure state $|\Psi_0\rangle$, and evolves unitarily under a quadratic Hamiltonian $\hat{H} = \sum_{i,j=1}^{V} h_{ij}\hat{c}_i^\dagger \hat{c}_j$, where $\hat{c}_i^\dagger$ ($\hat{c}_i$) creates (annihilates) a spinless fermion at site i, and V denotes the number of lattice sites. In what follows, we use uppercase (lowercase) Greek letters to denote quantum states in the many-body (single-particle) Hilbert space. One can diagonalize $\hat{H}$ via a unitary transformation of the creation and annihilation operators, $\hat{H} = \sum_\alpha \epsilon_\alpha \hat{f}_\alpha^\dagger \hat{f}_\alpha$. The single-particle energy eigenstates, with eigenenergies ϵ_α, can be written as $|\alpha\rangle \equiv \hat{f}_\alpha^\dagger|\emptyset\rangle$. The many-body energy eigenstates, with eigenenergies $E_\Omega = \sum_{\{\alpha\}} \epsilon_\alpha$, can be written as $|\Omega\rangle = \prod_{\{\alpha\}} \hat{f}_\alpha^\dagger|\emptyset\rangle$, where $\{\alpha\}$ is the set of N occupied $|\alpha\rangle$ for any given lattice filling $\overline{n} = N/V$. Any initial many-body pure state can be written as $|\Psi_0\rangle = \sum_\Omega \langle\Omega|\Psi_0\rangle|\Omega\rangle$.

Our focus is on one-body observables with rank $\mathbf{O}(1)$ [55], such as site and quasimomentum occupations, which are experimentally relevant and have the following form $\hat{O} = \sum_{\alpha\beta} O_{\alpha\beta}\hat{f}_\alpha^\dagger \hat{f}_\beta$ with $O_{\alpha\beta} = \langle\alpha|\hat{O}|\beta\rangle$. Their time evolution can be written in the many-body basis as $\langle\hat{O}(t)\rangle = \sum_\Omega \langle\Omega|e^{-i\hat{H}t}\hat{\rho}_0 e^{i\hat{H}t}\hat{O}|\Omega\rangle$, where $\hat{\rho}_0 = |\Psi_0\rangle\langle\Psi_0|$ is the density matrix of the initial state. In quadratic models, we can write it using the single-particle basis as

$$\langle\hat{O}(t)\rangle = \sum_\alpha \langle\alpha|e^{-i\hat{H}t}\hat{R}e^{i\hat{H}t}\hat{O}|\alpha\rangle = \sum_{\alpha,\beta=1}^{V} R_{\alpha\beta}O_{\beta\alpha}e^{i\omega_{\beta\alpha}t}, \tag{2}$$

where $\hat{R} = \sum_{\alpha\beta} R_{\alpha\beta}\hat{f}_\alpha^\dagger \hat{f}_\beta$ is the one-body density matrix of the initial state, with $R_{\alpha\beta} = \langle\Psi_0|\hat{f}_\beta^\dagger \hat{f}_\alpha|\Psi_0\rangle$ [56, 57], and $\omega_{\beta\alpha} = \epsilon_\beta - \epsilon_\alpha$.

The infinite time average of $\langle\hat{O}(t)\rangle$, for a non-degenerated single-particle spectrum, is given by

$$\overline{\langle\hat{O}(t)\rangle} \equiv \lim_{\tau\to\infty}\frac{1}{\tau}\int_0^\tau \langle\hat{O}(t)\rangle dt = \sum_\alpha O_{\alpha\alpha}R_{\alpha\alpha}. \tag{3}$$

The density matrix in the GGE is defined as $\hat{\rho}_{\rm GGE} = \frac{1}{Z_{\rm GGE}}e^{-\sum_\alpha \lambda_\alpha \hat{I}_\alpha}$ with $Z_{\rm GGE} = {\rm Tr}[e^{-\sum_\alpha \lambda_\alpha \hat{I}_\alpha}]$, the constants of motion being $\hat{I}_\alpha = \hat{f}_\alpha^\dagger \hat{f}_\alpha$, and the Lagrange multipliers fixed such that $R_{\alpha\alpha} = {\rm Tr}[\hat{\rho}_{\rm GGE}\hat{I}_\alpha]$. Therefore, the infinite-time average of $\langle\hat{O}(t)\rangle$ is reproduced by the GGE prediction [7, 35, 36]

$$\overline{\langle\hat{O}(t)\rangle} = \sum_\alpha O_{\alpha\alpha}{\rm Tr}[\hat{\rho}_{\rm GGE}\hat{I}_\alpha] = {\rm Tr}[\hat{\rho}_{\rm GGE}\hat{O}], \tag{4}$$

where we have used that $\hat{\rho}_{\rm GGE}$ is diagonal in the single-particle energy eigenbasis, so that ${\rm Tr}[\hat{\rho}_{\rm GGE}\sum_{\alpha\beta}O_{\alpha\beta}\hat{f}_\alpha^\dagger\hat{f}_\beta] = {\rm Tr}[\hat{\rho}_{\rm GGE}\sum_\alpha O_{\alpha\alpha}\hat{f}_\alpha^\dagger\hat{f}_\alpha]$.

Given that the infinite-time averages are guaranteed to be described by the GGE, all one needs for generalized thermalization to occur is the temporal fluctuations about the infinite-time average to vanish in the thermodynamic limit. The temporal fluctuations can be characterized by the variance [1]

$$\sigma_t^2 = \overline{\langle\hat{O}(t)\rangle^2} - \overline{\langle\hat{O}(t)\rangle}^2 . \tag{5}$$

Recall that the standard derivation of the upper bound for σ_t^2, which is based on the time evolution written in the many-body basis, requires that there are no gap degeneracies in the many-body spectrum [1]. This condition need not be fulfilled in quadratic models. The derivation that we provide below, which is based on Eq. (2), requires the absence of gap degeneracies in the single-particle spectrum. The latter is satisfied by QCQ Hamiltonians. Specifically, one can write

$$\overline{\langle\hat{O}(t)\rangle^2} = \sum_{\alpha,\beta,\omega,\rho} O_{\beta\alpha}O_{\rho\omega}R_{\alpha\beta}R_{\omega\rho}\overline{e^{i(\epsilon_\beta-\epsilon_\alpha+\epsilon_\rho-\epsilon_\omega)t}} . \tag{6}$$

which simplifies to (see Ref. [58])

$$\overline{\langle\hat{O}(t)\rangle^2} = \sum_{\alpha\neq\beta}|O_{\alpha\beta}|^2|R_{\alpha\beta}|^2 + \overline{\langle\hat{O}(t)\rangle}^2 , \tag{7}$$

We can therefore define the upper bound for the variance

$$\sigma_t^2 = \sum_{\alpha\neq\beta=1}^{V}|O_{\alpha\beta}|^2|R_{\alpha\beta}|^2 \leq \max\left\{|O_{\alpha\beta}|^2\right\}\sum_{\alpha=1}^{V}(R^2)_{\alpha\alpha} . \tag{8}$$

Since the eigenvalues of $\hat{R}$ belong to the interval $[0,1]$, one can replace $R^2 \to R$ in Eq. (8), and we obtain

$$\sigma_t^2 \leq \max\left\{V|O_{\alpha\beta}|^2\right\}\frac{1}{V}\sum_{\alpha=1}^{V}R_{\alpha\alpha} = \max\left\{V|O_{\alpha\beta}|^2\right\}\overline{n} , \tag{9}$$

where we used that $\sum_\alpha R_{\alpha\alpha} = \langle\psi_0|\sum_\alpha \hat{f}_\alpha^\dagger\hat{f}_\alpha|\psi_0\rangle = N$. Because the properly normalized one-body observables with rank $\mathbf{O}(1)$ can be written as $\hat{\mathcal{O}} \simeq \hat{O}\sqrt{V}$ [43], single-particle eigenstate thermalization in QCQ models results in $\max\left\{V|O_{\alpha\beta}|^2\right\} \propto 1/V$. Hence, the equilibration of these one-body observables is guaranteed in the thermodynamic limit. Notice that the polynomial scaling of the upper bound for σ_t^2 with the system size is independent of the details of the quantum quench, like the energy of the initial state $|\Psi_0\rangle$ or the filling factor $\overline{n}$. The above analysis can be extended to one-body operators that have rank $\mathbf{O}(V)$. Furthermore, in Ref. [58] we show that equilibration also occurs for q-body observables ($q = 2, 3, ...$) that are products of one-body observables, all of which exhibit single-particle eigenstate thermalization. Remarkably, our analysis applies to arbitrary initial states [58].

Numerical tests of equilibration. We consider local Hamiltonians that can be written as

$$\hat{H}_1 = -\sum_{\langle i,j\rangle}\hat{c}_i^\dagger\hat{c}_j + \sum_{i=1}^{V}\varepsilon_i\hat{c}_i^\dagger\hat{c}_i . \tag{10}$$

The first term describes hoppings between nearest neighbor sites, and ε_i is the onsite potential. We focus on

the 3D Anderson model on a cubic lattice with periodic boundary conditions, for which $\varepsilon_i = (W/2)r_i$ with r_i being a random number drawn from a uniform distribution in the interval $[-1, 1]$ [59]. We study dynamics in the two regimes of this model (which has a transition at $W_c \approx 16.5$ [60, 61]), at the $W = 5$ (delocalized, QCQ [42]) and $W = 25$ (localized) points. For the preparation of initial states in quantum quenches, which are always taken to be ground states in this work, we introduce a 3D superlattice model with $\varepsilon_i = \pm\mathcal{W}$ in Eq. (10), where the sign alternates between nearest neighbor sites. This 3D superlattice model allows us to create highly nonthermal distributions of momenta in the initial state (in the spirit of the quantum Newton's cradle experiment [62]). We complement our analysis with a quadratic model that is not quantum chaotic, i.e., 1D noninteracting fermions in a homogeneous lattice with open boundary conditions [$\varepsilon_i = 0$ in Eq. (10)]. To prepare the initial states for the quenches, we use the Aubry-André model [$\varepsilon_i = -\Lambda\cos(2\pi\sigma i)$ with $\sigma = (\sqrt{5}-1)/2$] in Eq. (10).

We also consider a paradigmatic nonlocal QCQ model, the SYK2 model in the Dirac fermion formulation [63],

$$\hat{H}_2 = \sum_{i,j=1}^{V} \left[(1-\gamma)a_{ij} + \gamma b_{ij}\right] \hat{c}_i^\dagger \hat{c}_j, \tag{11}$$

where the diagonal (off-diagonal) elements of the matrices $\mathbf{a}$ and $\mathbf{b}$ are real normally distributed random numbers with zero mean and $2/V$ ($1/V$) variance, while $\gamma \in [0, 1]$. The choice of an unconventional form of the SYK2 Hamiltonian (as a sum of two one-body operators) allows us to distinguish between weak and strong quantum quenches, as explained in Ref. [58].

In Fig. 1, we show results of numerical tests of equilibration for two observables, the occupation of a lattice site, $\hat{n}_1 = \hat{c}_1^\dagger \hat{c}_1$, and the occupation of the zero quasi-momentum mode, $\hat{m}_0 = \frac{1}{V}\sum_{ij} \hat{c}_i^\dagger \hat{c}_j$. Specifically, we plot the time evolution of $\langle \hat{O}(t)\rangle - \langle \hat{O}\rangle_{\rm GGE}$ in Figs. 1(a)–1(d), while the temporal fluctuations σ_t as functions of V are shown in Fig. 1(e). For the quench from the 3D superlattice model at $\mathcal{W} = 1$ to the 3D Anderson model at $W = 5$, see Figs. 1(a) and 1(b), the temporal fluctuations σ_t of both observables decrease with increasing system size, and a scaling $\sigma_t \propto V^{-\zeta}$ with $\zeta \approx 0.5$ is observed in Fig. 1(e). An exponent $\zeta = 0.5$ is expected because $\max\{V|O_{\alpha\beta}|^2\} \propto 1/V$ for those observables [43]. In contrast, for the quench from the 3D Anderson model at $W_0 = 30$ to the same model (with a different disorder realization) at $W = 25$ in Fig. 1(c) [Fig. 1(d)], the temporal fluctuations σ_t do not decrease (do decrease) with increasing system size for $\hat{n}_1$ ($\hat{m}_0$), and a scaling $\sigma_t \propto V^{-\zeta}$ with $\zeta \approx 0$ ($\zeta \approx 0.5$) is observed in Fig. 1(e). This a consequence of the fact that $\hat{m}_0$, but not $\hat{n}_1$, exhibits signatures of single-particle eigenstate thermalization in the localized regime of the 3D Anderson model [43]. Qualitatively similar results to those for $W = 25$ were reported in the presence of real-space localization in the 1D Anderson model [34, 35], and in the 1D Aubry-André model [13, 36].

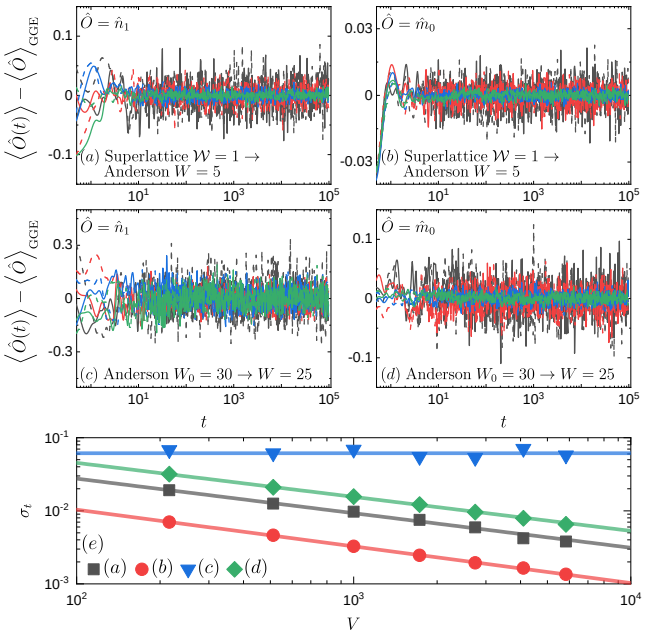

FIG. 1. (a)–(d) Time evolution of $\langle \hat{O}(t)\rangle - \langle \hat{O}\rangle_{\rm GGE}$ after quantum quenches in 3D models. The numerical results for system with $V = 6^3$, 8^3, 14^3, and 18^3 are marked with black, red, blue, and green, respectively. We show results for two (solid and dashed) quench realizations for each V. (a), (b) Quenches from the 3D superlattice model at $\mathcal{W} = 1$ and $\overline{n} = 1/4$ to the 3D Anderson model at $W = 5$. (c), (d) Quenches from the 3D Anderson model at $W_0 = 30$ and $\overline{n} = 1/2$ to the same model (with a different disorder realization) at $W = 25$. Two operators are considered (a), (c) $\hat{n}_1$ and (b), (d) $\hat{m}_0$. (e) Temporal fluctuations σ_t calculated within the time interval $t \in [10^2, 10^5]$ and averaged over 20 quench realizations. The lines show the outcome of two parameter fits κ/V^ζ. We get $\zeta \in [0.46, 0.5]$ for (a), (b), and (d).

Stationary state. Since eigenstate thermalization occurs in single-particle eigenstates of QCQ models, it is natural to wonder whether it also occurs in the many-body eigenstates of those models. If this is the case, the predictions of the GGE will be identical to those of the GE in the thermodynamic limit, $\langle \hat{O}\rangle_{\rm GGE} = \langle \hat{O}\rangle_{\rm GE}$, where $\langle \hat{O}\rangle_{\rm GGE} = {\rm Tr}[\hat{\rho}_{\rm GGE}\hat{O}]$ and $\langle \hat{O}\rangle_{\rm GE} = {\rm Tr}[\hat{\rho}_{\rm GE}\hat{O}]$, with $\hat{\rho}_{\rm GE} = \frac{1}{Z_{\rm GE}} e^{-\sum_\alpha (\epsilon_\alpha - \mu)/(k_B T)\, \hat{f}_\alpha^\dagger \hat{f}_\alpha}$, and $Z_{\rm GE} = {\rm Tr}[e^{-\sum_\alpha (\epsilon_\alpha - \mu)/(k_B T)\hat{f}_\alpha^\dagger \hat{f}_\alpha}]$. k_B, T, and μ are the Boltzmann constant, the temperature, and the chemical potential, respectively.

We address this question in the context of the quenches to the 3D Anderson model with $W = 5$. We focus on $\hat{m}_0$. The finite-size scaling of the difference $|\Delta\langle \hat{m}_0\rangle| = |\langle \hat{m}_0\rangle_{\rm GGE} - \langle \hat{m}_0\rangle_{\rm GE}|$ is reported in Fig. 2. Each point was calculated for a single quench realization, and then averaged over 100 quench realizations. It is apparent that the difference $|\Delta\langle \hat{m}_0\rangle|$ rapidly converges to a nonzero value. Therefore, the GGE is expected to be different from the

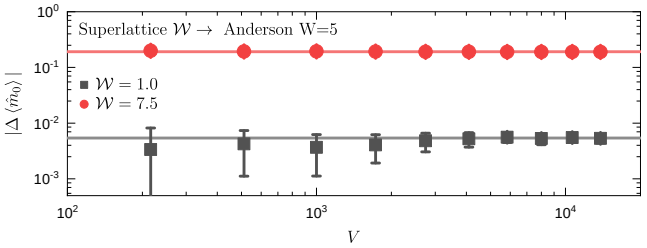

FIG. 2. Finite-size scaling of the difference $|\Delta\langle\hat{m}_0\rangle|$ for quenches from the 3D superlattice model with $\mathcal{W}\in\{1,7.5\}$ and $\overline{n}=1/4$ to the 3D Anderson model with $W=5$. Horizontal lines mark the mean values for the five largest system sizes $V\in\{16^3,\ ...,\ 24^3\}$. The results were averaged over $M=100$ quench realizations. The error bars are standard deviations $\sigma=\left(\sum_{i=1}^{M}|\Delta\langle\hat{m}_0\rangle|_i^2/M-(\sum_{i=1}^{M}|\Delta\langle\hat{m}_0\rangle|_i/M)^2\right)^{1/2}$.

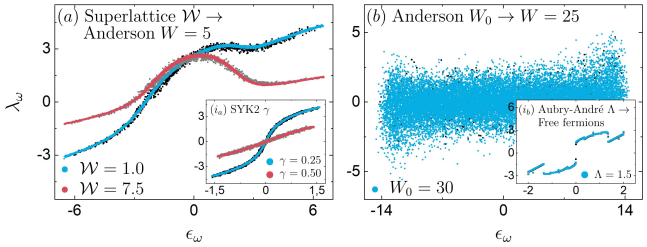

FIG. 3. Lagrange multipliers λ_α plotted versus single-particle energies ϵ_α. Black and gray (blue and red) points depict results for $V=10^3$ ($V=28^3$) and a single quench realization. These quenches are: (a) the 3D superlattice model with $\mathcal{W}=1$ and 7.5 to the 3D Anderson model with $W=5$ (main panel), and the change of $\mathbf{b}$ to a new random realization in the SYK2 model with $\gamma=0.25$ and 0.5 (inset); (b) the 3D Anderson model at $W_0=30$ to the same model (with a different disorder realization) at $W=25$ (main panel), and the Aubry-André model with $\Lambda=1.5$ to free fermions (inset). In all cases $\overline{n}=1/2$, except for the main panel in (a) where $\overline{n}=1/4$.

GE in the thermodynamic limit. (Qualitatively similar results as in this section and the previous one were obtained for other models, quenches and observables.)

Absence of eigenstate thermalization in many-body energy eigenstates. The numerical results from the previous section suggest that the many-body eigenstates of QCQ Hamiltonians do not exhibit eigenstate thermalization [the infinite time averages from Eq. (3) disagree with the predictions of the GE]. We can understand this analytically as follows (see Ref. [58] for a proof).

The diagonal matrix elements of $\hat{O}$ in the many-body energy eigenstates $|\Omega\rangle$ can be written as

$$\langle\Omega|\hat{O}|\Omega\rangle=\sum_{\alpha,\beta=1}^{V}O_{\alpha\beta}\langle\Omega|\hat{f}_\alpha^\dagger\hat{f}_\beta|\Omega\rangle=\sum_{\alpha=1}^{V}O_{\alpha\alpha}\langle\Omega|\hat{f}_\alpha^\dagger\hat{f}_\alpha|\Omega\rangle\ , \tag{12}$$

where the expectation values $\langle\Omega|\hat{f}_\alpha^\dagger\hat{f}_\alpha|\Omega\rangle$ are equal 0 or 1. Hence, the behavior of the diagonal many-body matrix elements [and so the infinite time averages from Eq. (3)] is governed by an extensive (in V) sum of the diagonal single-particle matrix elements $O_{\alpha\alpha}$.

The diagonal matrix elements $O_{\alpha\alpha}$ exhibit $\mathbf{O}(1/V)$ fluctuations about their smooth function $\mathcal{O}(\epsilon_\alpha)$ [43]. For simplicity, let us consider $\mathcal{O}(\epsilon_\alpha)=0$. We can build many-body eigenstates $|\Omega\rangle$, for which V/a and V/b of $O_{\alpha\alpha}\langle\Omega|\hat{f}_\alpha^\dagger\hat{f}_\alpha|\Omega\rangle$ are positive and negative, respectively. The corresponding diagonal matrix elements read

$$\langle\Omega|\hat{O}|\Omega\rangle=\sum_{\beta=1}^{V/a}|O_{\beta\beta}|-\sum_{\beta=1}^{V/b}|O_{\beta\beta}|\sim\left(\frac{V}{a}-\frac{V}{b}\right)\mathbf{O}\left(\frac{1}{V}\right), \tag{13}$$

where $1/a+1/b=\overline{n}$. These diagonal matrix elements are $\mathbf{O}(1)$ when $a\neq b$, so they do not approach the microcanonical average in the thermodynamic limit. Furthermore, the number of such many-body states increases exponentially with the system size

$$\mathcal{N}=\binom{V/2}{V/a}\binom{V/2}{V/b}\geq\left[\frac{V/2}{V/a}\right]^{\frac{V}{a}}\left[\frac{V/2}{V/b}\right]^{\frac{V}{b}}=2^{\kappa V}\ , \tag{14}$$

where we have introduced $\kappa=\frac{1}{a}\log_2\left(\frac{a}{2}\right)+\frac{1}{b}\log_2\left(\frac{b}{2}\right)$.

Smoothness of Lagrange multipliers. To conclude, let us explore the properties of the GGE in QCQ Hamiltonians. Note that whenever the Lagrange multipliers are linear functions of the single-particle energies, i.e., $\lambda_\alpha=(\epsilon_\alpha-\mu)/(k_BT)$, the GGE is the same as the GE.

The Lagrange multipliers λ_α are plotted as functions of the single-particle energies ϵ_α in Fig. 3(a) for quenches in which the final Hamiltonian exhibits single-particle quantum chaos: the 3D Anderson model with $W=5$ (main panel) and the SYK2 model (inset). It is notable that λ_α are smooth functions of ϵ_α, and that they are not linear in ϵ_α, even in the quench within the SYK2 model with an arbitrary $\gamma<1$ (the exception is $\gamma=1$, which is at "infinite temperature", see Ref. [58]). In Fig. 3(b), we plot the Lagrange multipliers λ_α vs ϵ_α for quenches in which the final Hamiltonian does not exhibit single-particle quantum chaos: the 3D Anderson model in the localized regime with $W=25$ (main panel) and 1D non-interacting fermions in a homogeneous potential (inset). In the former, λ_α exhibits fluctuations that do not appear to vanish when increasing system size V, while in the latter λ_α exhibits jumps. In Ref. [58], we quantify the eigenstate-to-eigenstate fluctuations $\delta\lambda_\alpha=\lambda_\alpha-\lambda_{\alpha-1}$, and show numerically and analitically that λ_α is a smooth function of ϵ_α for QCQ Hamiltonians.

Summary. Generalized thermalization is expected to occur for interacting integrable models. Here we proved that it is guaranteed to occur for quadratic Hamiltonians that exhibit single-particle eigenstate thermalization, namely, for QCQ Hamiltonians. Furthermore, we showed that the many-body eigenstates of QCQ Hamiltonians do not exhibit eigenstate thermalization. Consequently, the GGE is generally needed to describe the expectation values of observables after equilibration, and we showed that it is characterized by Lagrange multipliers that are smooth functions of the single-particle energies.

ACKNOWLEDGMENTS

We acknowledge the support of the National Science Centre, Poland via project 2020/37/B/ST3/00020 (M.M.), the National Science Foundation, Grant No. 2012145 (M.R.), and the Slovenian Research Agency (ARRS), Research Core Fundings Grants P1-0044 and J1-1696 (L.V.).

[1] L. D'Alessio, Y. Kafri, A. Polkovnikov, and M. Rigol, From quantum chaos and eigenstate thermalization to statistical mechanics and thermodynamics, Adv. Phys. **65**, 239 (2016).

[2] J. Eisert, M. Friesdorf, and C. Gogolin, Quantum many-body systems out of equilibrium, Nat. Phys. **11**, 124 (2015).

[3] T. Mori, T. N. Ikeda, E. Kaminishi, and M. Ueda, Thermalization and prethermalization in isolated quantum systems: a theoretical overview, J. Phys. B **51**, 112001 (2018).

[4] J. M. Deutsch, Eigenstate thermalization hypothesis, Rep. Prog. Phys. **81**, 082001 (2018).

[5] M. Rigol, V. Dunjko, and M. Olshanii, Thermalization and its mechanism for generic isolated quantum systems, Nature (London) **452**, 854 (2008).

[6] M. Rigol, V. Dunjko, V. Yurovsky, and M. Olshanii, Relaxation in a completely integrable many-body quantum system: An ab initio study of the dynamics of the highly excited states of 1D lattice hard-core bosons, Phys. Rev. Lett. **98**, 050405 (2007).

[7] L. Vidmar and M. Rigol, Generalized Gibbs ensemble in integrable lattice models, J. Stat. Mech. (2016), 064007.

[8] M. A. Cazalilla, Effect of suddenly turning on interactions in the Luttinger model, Phys. Rev. Lett. **97**, 156403 (2006).

[9] M. Rigol, A. Muramatsu, and M. Olshanii, Hard-core bosons on optical superlattices: Dynamics and relaxation in the superfluid and insulating regimes, Phys. Rev. A **74**, 053616 (2006).

[10] A. Iucci and M. A. Cazalilla, Quantum quench dynamics of the Luttinger model, Phys. Rev. A **80**, 063619 (2009).

[11] A. C. Cassidy, C. W. Clark, and M. Rigol, Generalized thermalization in an integrable lattice system, Phys. Rev. Lett. **106**, 140405 (2011).

[12] P. Calabrese, F. H. L. Essler, and M. Fagotti, Quantum quench in the transverse-field Ising chain, Phys. Rev. Lett. **106**, 227203 (2011).

[13] C. Gramsch and M. Rigol, Quenches in a quasidisordered integrable lattice system: Dynamics and statistical description of observables after relaxation, Phys. Rev. A **86**, 053615 (2012).

[14] P. Calabrese, F. H. L. Essler, and M. Fagotti, Quantum quenches in the transverse field Ising chain: II. stationary state properties, J. Stat. Mech. **2012**, P07022 (2012).

[15] F. H. L. Essler, S. Evangelisti, and M. Fagotti, Dynamical Correlations After a Quantum Quench, Phys. Rev. Lett. **109**, 247206 (2012).

[16] J.-S. Caux and F. H. L. Essler, Time evolution of local observables after quenching to an integrable model, Phys. Rev. Lett. **110**, 257203 (2013).

[17] J.-S. Caux and R. M. Konik, Constructing the generalized Gibbs ensemble after a quantum quench, Phys. Rev. Lett. **109**, 175301 (2012).

[18] M. Kormos, A. Shashi, Y.-Z. Chou, J.-S. Caux, and A. Imambekov, Interaction quenches in the one-dimensional Bose gas, Phys. Rev. B **88**, 205131 (2013).

[19] B. Pozsgay, The generalized Gibbs ensemble for Heisenberg spin chains, J. Stat. Mech. **2013**, P07003 (2013).

[20] M. Fagotti, M. Collura, F. H. L. Essler, and P. Calabrese, Relaxation after quantum quenches in the spin-$\frac{1}{2}$ Heisenberg XXZ chain, Phys. Rev. B **89**, 125101 (2014).

[21] J. De Nardis, B. Wouters, M. Brockmann, and J.-S. Caux, Solution for an interaction quench in the Lieb-Liniger Bose gas, Phys. Rev. A **89**, 033601 (2014).

[22] B. Wouters, J. De Nardis, M. Brockmann, D. Fioretto, M. Rigol, and J.-S. Caux, Quenching the anisotropic Heisenberg chain: Exact solution and generalized Gibbs ensemble predictions, Phys. Rev. Lett. **113**, 117202 (2014).

[23] B. Pozsgay, M. Mestyán, M. A. Werner, M. Kormos, G. Zaránd, and G. Takács, Correlations after quantum quenches in the XXZ spin chain: Failure of the generalized Gibbs ensemble, Phys. Rev. Lett. **113**, 117203 (2014).

[24] M. Mierzejewski, P. Prelovšek, and T. Prosen, Identifying local and quasilocal conserved quantities in integrable systems, Phys. Rev. Lett. **114**, 140601 (2015).

[25] E. Ilievski, M. Medenjak, and T. Prosen, Quasilocal conserved operators in the isotropic Heisenberg spin-1/2 chain, Phys. Rev. Lett. **115**, 120601 (2015).

[26] E. Ilievski, J. De Nardis, B. Wouters, J.-S. Caux, F. H. L. Essler, and T. Prosen, Complete generalized Gibbs ensembles in an interacting theory, Phys. Rev. Lett. **115**, 157201 (2015).

[27] L. Piroli, E. Vernier, P. Calabrese, and M. Rigol, Correlations and diagonal entropy after quantum quenches in XXZ chains, Phys. Rev. B **95**, 054308 (2017).

[28] M. Fagotti, V. Marić, and L. Zadnik, Nonequilibrium symmetry-protected topological order: emergence of semilocal Gibbs ensembles, arXiv:2205.02221.

[29] P. Calabrese, F. H. L. Essler, and G. Mussardo, Introduction to 'quantum integrability in out of equilibrium systems', J. Stat. Mech. **2016**, 064001 (2016).

[30] B. Bertini, M. Collura, J. De Nardis, and M. Fagotti, Transport in out-of-equilibrium XXZ chains: Exact profiles of charges and currents, Phys. Rev. Lett. **117**, 207201 (2016).

[31] O. A. Castro-Alvaredo, B. Doyon, and T. Yoshimura, Emergent hydrodynamics in integrable quantum systems out of equilibrium, Phys. Rev. X **6**, 041065 (2016).

[32] M. Schemmer, I. Bouchoule, B. Doyon, and J. Dubail, Generalized hydrodynamics on an atom chip, Phys. Rev. Lett. **122**, 090601 (2019).

[33] N. Malvania, Y. Zhang, Y. Le, J. Dubail, M. Rigol, and D. S. Weiss, Generalized hydrodynamics in strongly interacting 1D Bose gases, Science **373**, 1129 (2021).

[34] S. Ziraldo, A. Silva, and G. E. Santoro, Relaxation dynamics of disordered spin chains: Localization and the

existence of a stationary state, Phys. Rev. Lett. **109**, 247205 (2012).
[35] S. Ziraldo and G. E. Santoro, Relaxation and thermalization after a quantum quench: Why localization is important, Phys. Rev. B **87**, 064201 (2013).
[36] K. He, L. F. Santos, T. M. Wright, and M. Rigol, Single-particle and many-body analyses of a quasiperiodic integrable system after a quench, Phys. Rev. A **87**, 063637 (2013).
[37] T. M. Wright, M. Rigol, M. J. Davis, and K. V. Kheruntsyan, Nonequilibrium dynamics of one-dimensional hard-core anyons following a quench: Complete relaxation of one-body observables, Phys. Rev. Lett. **113**, 050601 (2014).
[38] M. Cramer, C. M. Dawson, J. Eisert, and T. J. Osborne, Exact relaxation in a class of nonequilibrium quantum lattice systems, Phys. Rev. Lett. **100** (2008).
[39] M. Gluza, C. Krumnow, M. Friesdorf, C. Gogolin, and J. Eisert, Equilibration via Gaussification in fermionic lattice systems, Phys. Rev. Lett. **117** (2016).
[40] C. Murthy and M. Srednicki, Relaxation to gaussian and generalized gibbs states in systems of particles with quadratic hamiltonians, Phys. Rev. E **100**, 012146 (2019).
[41] M. Gluza, J. Eisert, and T. Farrelly, Equilibration towards generalized Gibbs ensembles in non-interacting theories, SciPost Physics **7** (2019).
[42] P. Łydżba, M. Rigol, and L. Vidmar, Entanglement in many-body eigenstates of quantum-chaotic quadratic Hamiltonians, Phys. Rev. B **103**, 104206 (2021).
[43] P. Łydżba, Y. Zhang, M. Rigol, and L. Vidmar, Single-particle eigenstate thermalization in quantum-chaotic quadratic Hamiltonians, Phys. Rev. B **104**, 214203 (2021).
[44] J. Šuntajs, T. Prosen, and L. Vidmar, Spectral properties of three-dimensional Anderson model, Annals of Physics 168469 (2021).
[45] I. Ulčakar and L. Vidmar, Tight-binding billiards, Phys. Rev. E **106**, 034118 (2022).
[46] P. Łydżba, M. Rigol, and L. Vidmar, Eigenstate entanglement entropy in random quadratic Hamiltonians, Phys. Rev. Lett. **125**, 180604 (2020).
[47] C. Liu, X. Chen, and L. Balents, Quantum entanglement of the Sachdev-Ye-Kitaev models, Phys. Rev. B **97**, 245126 (2018).
[48] B. Al'tshuler and B. Shklovskii, Repulsion of energy levels and conductivity of small metal sample, Zh. Eksp. Teor. Fiz. **91**, 220 (1986).
[49] B. Al'tshuler, I. Zharekeshev, S. Kotochigova, and B. Shklovskii, Repulsion between energy levels and the metal-insulator transition, Zh. Eksp. Teor. Fiz. **94**, 343 (1988).
[50] Namely, for lattice systems such as the ones of interest here, satisfying $\frac{1}{V}\mathrm{Tr}\{\hat{\mathcal{O}}^2\} = 1$, where V is the number of lattice sites.
[51] M. Srednicki, The approach to thermal equilibrium in quantized chaotic systems, J. Phys. A. **32**, 1163 (1999).
[52] E. Bianchi, L. Hackl, and M. Kieburg, Page curve for fermionic Gaussian states, Phys. Rev. B **103**, L241118 (2021).
[53] E. Bianchi, L. Hackl, M. Kieburg, M. Rigol, and L. Vidmar, Volume-Law Entanglement Entropy of Typical Pure Quantum States, PRX Quantum **3**, 030201 (2022).
[54] M. Lucas, L. Piroli, J. De Nardis, and A. De Luca, Generalized deep thermalization for free fermions, arXiv:2207.13628.
[55] Namely, observables that have an $\mathbf{O}(1)$ number of non-degenerate eigenvalues in the single-particle spectrum.
[56] L. C. Venuti and P. Zanardi, Gaussian equilibration, Phys. Rev. E **87**, 012106 (2013).
[57] L. C. Venuti, Theory of temporal fluctuations in isolated quantum systems, *Quantum Criticality in Condensed Matter* (WORLD SCIENTIFIC, 2015).
[58] See Supplemental Material for the derivation of Eq. (8), equilibration of q-body observables, absence of ETH in many-body energy eigenstates, details on the GGE in the SYK2 model, the difference between the GGE and GE in the 3D Anderson model, and the smoothness of Lagrange multipliers. It includes Refs. [67–70].
[59] P. W. Anderson, Absence of diffusion in certain random lattices, Phys. Rev. **109**, 1492 (1958).
[60] K. Slevin and T. Ohtsuki, Critical exponent for the anderson transition in the three-dimensional orthogonal universality class, New Journal of Physics **16**, 015012 (2014).
[61] K. Slevin and T. Ohtsuki, Critical exponent of the Anderson transition using massively parallel supercomputing, J. Phys. Soc. Jpn. **87**, 094703 (2018).
[62] T. Kinoshita, T. Wenger, and S. D. Weiss, A quantum Newton's cradle, Nature (London) **440**, 900 (2006).
[63] S. Sachdev and J. Ye, Gapless spin-fluid ground state in a random quantum heisenberg magnet, Phys. Rev. Lett. **70**, 3339 (1993).
[64] M. A. Cazalilla, A. Iucci, and M.-C. Chung, Thermalization and quantum correlations in exactly solvable models, Phys. Rev. E **85**, 011133 (2012).
[65] T. Kita, *Density Matrices and Two-Particle Correlations*, *Statistical Mechanics of Superconductivity*, 61–71 (Springer Japan, Tokyo, 2015).
[66] C. N. Yang, Concept of off-diagonal long-range order and the quantum phases of liquid he and of superconductors, Rev. Mod. Phys. **34**, 694 (1962).
[67] M. Haque and P. A. McClarty, Eigenstate thermalization scaling in Majorana clusters: From chaotic to integrable Sachdev-Ye-Kitaev models, Phys. Rev. B **100**, 115122 (2019).
[68] M. Rigol and M. Fitzpatrick, Initial-state dependence of the quench dynamics in integrable quantum systems, Phys. Rev. A **84**, 033640 (2011).
[69] K. He and M. Rigol, Initial-state dependence of the quench dynamics in integrable quantum systems. ii. thermal states, Phys. Rev. A **85**, 063609 (2012).
[70] K. He and M. Rigol, Initial-state dependence of the quench dynamics in integrable quantum systems. iii. chaotic states, Phys. Rev. A **87**, 043615 (2013).
[71] The traceless normalized operator corresponding to $\hat{o}_n$ has the form $\underline{\hat{o}}_n = \frac{1}{\sqrt{V-1}}(V\hat{o}_n - 1)$, for which $\delta(\underline{o}_n)_\alpha \propto 1/\sqrt{V}$ [43, 58].